Cellular correlates of cortical thinning throughout the lifespan

Vidal-Pineiro, D. PhD[1], Parker, N., M.Sc.[2,3], Shin, J. PhD[4], French, L. PhD[5], Jackowski, AP. MD/PhD[6,7], Mowinckel, AM. PhD[1], Patel, Y.[2,3], Pausova, Z., MD[4], Salum, G. MD/PhD[7,8], Sørensen, Ø., PhD[1], Walhovd, KB PhD[1,9], Paus, T., MD/PhD[2,3,10]*, Fjell, AM PhD[1,9]*, and the Australian Imaging Biomarkers and Lifestyle flagship study of ageing[&]

[1]Centre for Lifespan Changes in Brain and Cognition, Department of Psychology, University of Oslo, Oslo, Norway.

[2]Bloorview Research Institute, Holland Bloorview Kids Rehabilitation Hospital, Toronto, ON, Canada;

[3]Institute of Medical Science, University of Toronto, Toronto, ON, Canada

[4]The Hospital for Sick Children, University of Toronto, Toronto, ON, Canada;

[5]Centre for Addiction and Mental Health, University of Toronto, Toronto, ON, Canada

[6]Interdisciplinary Lab for Clinical Neurosciences (LiNC), University Federal of São Paulo, Brazil

[7]National Institute of Developmental Psychiatry for Children and Adolescents (INCT-CNPq), São Paulo, Brazil

[8]Department of Psychiatry, Federal University of Rio Grande do Sul, Porto Alegre, Brazil

[9]Department of radiology and nuclear medicine, Oslo University Hospital, Oslo, Norway

[10]Departments of Psychology and Psychiatry, University of Toronto, ON, Canada

[&]Data used in the preparation of this article were partially obtained from the Australian Imaging Biomarkers and Lifestyle flagship study of ageing (AIBL) funded by the Commonwealth Scientific and Industrial Research Organisation (CSIRO), which was made available at the ADNI database (www.loni.usc.edu/ADNI). The AIBL researchers contributed data but did not participate in analysis or writing of this report. AIBL researchers are listed at www.aibl.csiro.au.

*Denotes equal contribution and corresponding authors

Corresponding authors:

Tomáš Paus

Bloorview Research Institute, 150 Kilgour Road

Toronto, Ontario, Canada, M4G 1R8

tpaus@hollandbloorview.ca

Tel: (416) 425-6220, extension 6023

Fax: 416 525 6591

Anders Martin Fjell

Department of Psychology, Pb. 1094 Blindern

Oslo, Norway, 0317

a.m.fjell@psykologi.uio.no

Tel: (+47)-22845129

Abstract

Changes in cortical thickness occur throughout the lifespan, but the neurobiological substrates are poorly understood. Here, we compared the regional patterns of cortical thinning (Magnetic Resonance Images; >4000 observations) with those of gene expression for several neuronal and non-neuronal cell types (Allen Human Brain Atlas). Inter-regional profiles of cortical thinning (estimated from MRIs) related to expression profiles for marker genes of CA1 pyramidal cells, astrocytes and microglia during development (less thinning, greater gene expression). The same expression – thinning patterns were mirrored in aging, but in the opposite direction. The results were replicated in independent MRI datasets. Further analyses suggested that the cell type – thinning relationship is facilitated by astrocytic metabolic processes in development and neural projection and synaptic changes in aging. Overall, these findings uncover the neurobiological mechanisms underlying cortical thinning across the lifespan and may contribute to our understanding of the molecular pathways involved in neurodevelopmental and neurodegenerative disorders.

Introduction

The human cerebral cortex undergoes constant remodeling throughout the lifespan. Magnetic resonance imaging (MRI) enables the estimation of structural properties of the human cerebral cortex that can, in turn, be related to cognitive, clinical and demographic data [1–4], and used as high-fidelity phenotypes for genomic studies [4–6]. Yet, we lack data necessary for guiding interpretation of MRI-based phenotypes with regard to the underlying neurobiology [7,8]. Relating MRI-based changes in cortical thickness to specific neurobiological processes is fundamental for our understanding of the normal lifespan trajectories and individual differences of cortical thickness, as well as the nature of cortical abnormalities of various neurodevelopmental and neurodegenerative disorders. Here, we approach this question by studying the regional patterns of age-related cortical thinning in relation to those of mRNA expression of genes indexing several neuronal and non-neuronal cell types.

For MRI-based estimates of cortical thickness, the prototypic lifespan trajectory includes a steep age-related decrease in childhood and adolescence, followed by a mild monotonic thinning from early adulthood, and in many regions, an accelerated thinning from about the seventh decade of life [9–11]. Despite uninterrupted cortical thinning during the lifespan, the underlying neurobiological substrates and processes must be different. Developmental changes in cortical thickness may involve processes such as intracortical myelination, remodeling of dendritic arbours and its components (e.g., dendritic spines), axonal sprouting, and vascularization [12–16]. With advancing age, cortical thinning may, for instance, be associated with neuronal and dendritic shrinkage [17–19]. Similar changes at different ages can be related to different biological processes. This may be one of the reasons why the relationship between cognition and cortical thinning tends to exhibit different directions in different age periods: negative in older age (less thinning, better cognition) and positive in childhood and adolescence (more thinning, better cognition) [20,21]. Altogether, it seems either that the neurobiological foundations of

cortical thinning estimated from MRI differ across age periods or that the same components are affected in different directions throughout the lifespan.

The human cerebral cortex consists on several types of cells, which can be classified into neuronal – mostly pyramidal cells and interneurons - and non-neuronal cells - mostly glial cells, namely microglia, astrocytes and oligodendrocytes [22–24]. Histological data suggest that regional variations of cortical thickness may be associated with the number of non-neuronal cells and neuropil volume [25,26]. Yet, this *ex vivo* approach may be less suited to uncover the microstructural substrate driving age-related changes in cortical thickness in the general population. Two recent studies have addressed this issue [27,28] by combining cross-sectional estimates of cortical thickness during adolescence with quantitative MRI data and gene expression data. By combining magnetization transfer and cortical thickness estimates, Whitaker et al. [27] suggested intra-cortical myelination as a primary driver of cortical thinning in the adolescent cortex. On the other side, Shin et al. [28] combined regional profiles of age-related cortical thickness in adolescence and cell-specific gene expression. Their results suggested that – across the cerebral cortex – inter-regional variations in cortical thinning are associated (negatively) with inter-regional variations in the expression of marker genes for CA1 pyramidal cells, astrocytes, and microglia.

Here we ask whether age-related changes in thickness of the human cerebral cortex, assessed *in vivo* with longitudinal MRI, are associated with specific neuronal or non-neuronal cell-types. We approached this question using virtual histology [28], namely by correlating regional profiles of cortical thinning – during different periods of the lifespan - with regional profiles of cell-specific gene expression. Further, to understand the biological processes that articulate the cell type – cortical thinning relationship during a given period in life, we identified those processes that were associated with a specific cell-type, regulated during the given age period and linked with cortical thinning. Our

objective was to shed light on the neurobiological substrates underlying cortical thinning at different stages during the lifespan, and the molecular mechanisms that mediate the cell type – cortical thinning relationship at different age periods.

Site	Obs.	Participants	Obs./participant (mean)	Sex (f:m)	Age (SD)	Age range
LCBC (all)	4,004	1,899	2.1	1,135:764	37.4 (25.3)	4.1 - 89.4
Skyra 3.0 T	1,934	1,081	1.8	684:397	46.0 (23.3)	8.5 - 89.4
Avanto1 1.5 T	240	135	1.8	67:69	8.6 (1.4)	4.9 - 12.1
Avanto2 1.5 T	1,737	875	2.0	470:405	32.1 (25.1)	4.1 - 89.4
Prisma 3.0 T	93	93	1	68:25	33.5 (11.3)	20.5 - 70.3

Table 1*. MRI sample descriptives. Main sociodemographic information of the MRI sample, also grouped by scanner. Obs. = Observations, f:m = female:male.*

Briefly, the MRI and gene expression datasets were parsed into 34 cortical regions-of-interest (ROIs) of the left hemisphere [29]. MRI data were drawn from the Center for Lifespan Changes in Brain and Cognition (LCBC) consisting of 4,004 observations from 1,899 cognitively healthy participants with up to 6 time points each (**Table 1**). MRI data were processed through the FreeSurfer pipeline and fitted using generalized additive mixed models (GAMM) (see **Materials and methods** for details). Cortical thinning was estimated as the first derivative of the fitted model, and units represent mm of thickness change per year (mm/yr). For gene expression, we used the Allen Human Brain Atlas (AHBA) [30], a public resource that includes values of gene expression in multiple regions of the human cerebral cortex. As cell-specific markers, we used genes identified as unique to one of nine cell-types based on single-cell RNA data extracted from the CA1 region and the somatosensory region (S1) in mice [31]. Genes without consistent inter-regional profiles of their expression were filtered out [28]. As most cortical regions show thinning during the whole lifespan, hereafter we refer to the cortical thinning/thickening estimates by cortical thinning and use the terms “more and less thinning” to denote directionality. Note though that the cortical estimates are measured throughout the thickening/thinning continuum and positive values in the derivative reflect thickening while negative values denote thinning.

Results

Lifespan trajectories of cortical thickness and cortical thinning.

For most regions, the lifespan trajectories of cortical thickness displayed the prototypic pattern characterized by a steep decline in MRI-based estimates of thickness during childhood and adolescence, a mild monotonic thinning from the early adulthood onwards, and a trend towards accelerated thinning in older adulthood as shown by the first derivatives of the fitting (see **Fig. 1)**. See an interactive visualization of cortical thickness and thinning trajectories for each region in **supporting information.**

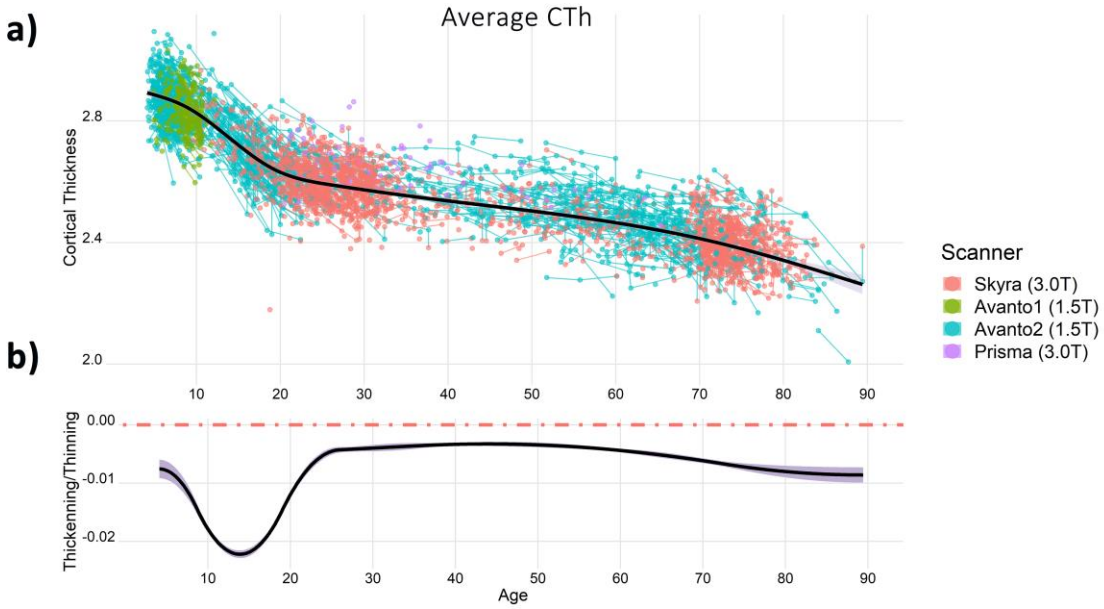

Figure 1. *Trajectories of average cortical thickness. The upper and lower plots exhibit the trajectories of cortical thickness and cortical thinning during the lifespan, respectively. Cortical thickness fitting (black line) overlies a spaghetti plot that displays each observation (dots), participant (thin lines) and, scanner (color). The y-axis units represent mm and mm/year for the thickness and thinning plots, respectively. The dotted red line in the cortical thinning graph represents 0 change, negative and positive values represent thinning and thickening, respectively.*

Lifespan Virtual Histology. Cell type – cortical thinning relationship throughout the lifespan.

Next, we used the virtual-histology approach to assess the relationship between cortical thinning across the lifespan (first-derivative) and cell-specific gene expression across the 34 cortical regions. As shown in **Fig. 2a,** we observed that the average correlation coefficient for the different cell-types varied throughout the lifespan. The average correlation coefficients differed from the empirical null distributions for the following cell-types and age periods: astrocytes (5 - 11 years, 35 – 41 years, 61 - 67 years), microglia (5 - 13 years, 65 - 71 years) and CA1 pyramidal cells (5 - 9 years, 63 - 79 years). All results were corrected for both the within (Bonferroni) and between (FDR) cell-type multiple comparisons. Note that the first derivative denotes the degree of thinning so that regions with lower thinning have less negative values of the first derivative. Therefore, a positive correlation implies that – across the 34 cortical regions - the higher the cell-specific gene expression values are, the less steep the cortical thinning is (i.e., less negative first derivative). Conversely, for a negative correlation: the higher the cell-type expression values are, the steeper (i.e., more negative 1st derivative) the cortical thinning. The average correlation coefficients in childhood/adolescence (for astrocytes, microglia and, CA1 pyramidal cells), and during middle-age (for astrocytes) were positive: thus, cortical regions with higher cell-specific expression for astrocytes, microglia, and CA1 pyramidal cells displayed *less* pronounced thinning. During older age, the gene expression – thinning correlations were negative: thus, cortical regions with higher cell-specific expression for astrocytes, microglia and, CA1 pyramidal cells displayed *more* pronounced age-related cortical thinning. The results were robust to variations of different fitting parameters (**SI text; Supplementary Fig. 1**). The complete statistics are available in the **supporting information.** Next, we replicated the main findings in three independent datasets that corresponded to the age periods with significant results (i.e. childhood/adolescence, middle-age and older age periods). As seen in **Fig. 2b**, we replicated all expression – thinning correlations observed in the discovery sample: positive correlations for astrocytes, microglia and CA1 pyramidal cells in childhood and adolescence, positive correlation for astrocytes in middle-age, and negative

correlations for astrocytes, microglia and CA1 pyramidal cells in older age. Note that significance was only tested for the cell types that were significant in the main (discovery) results. See **SI text** for a detailed description of the replication results and the samples used.

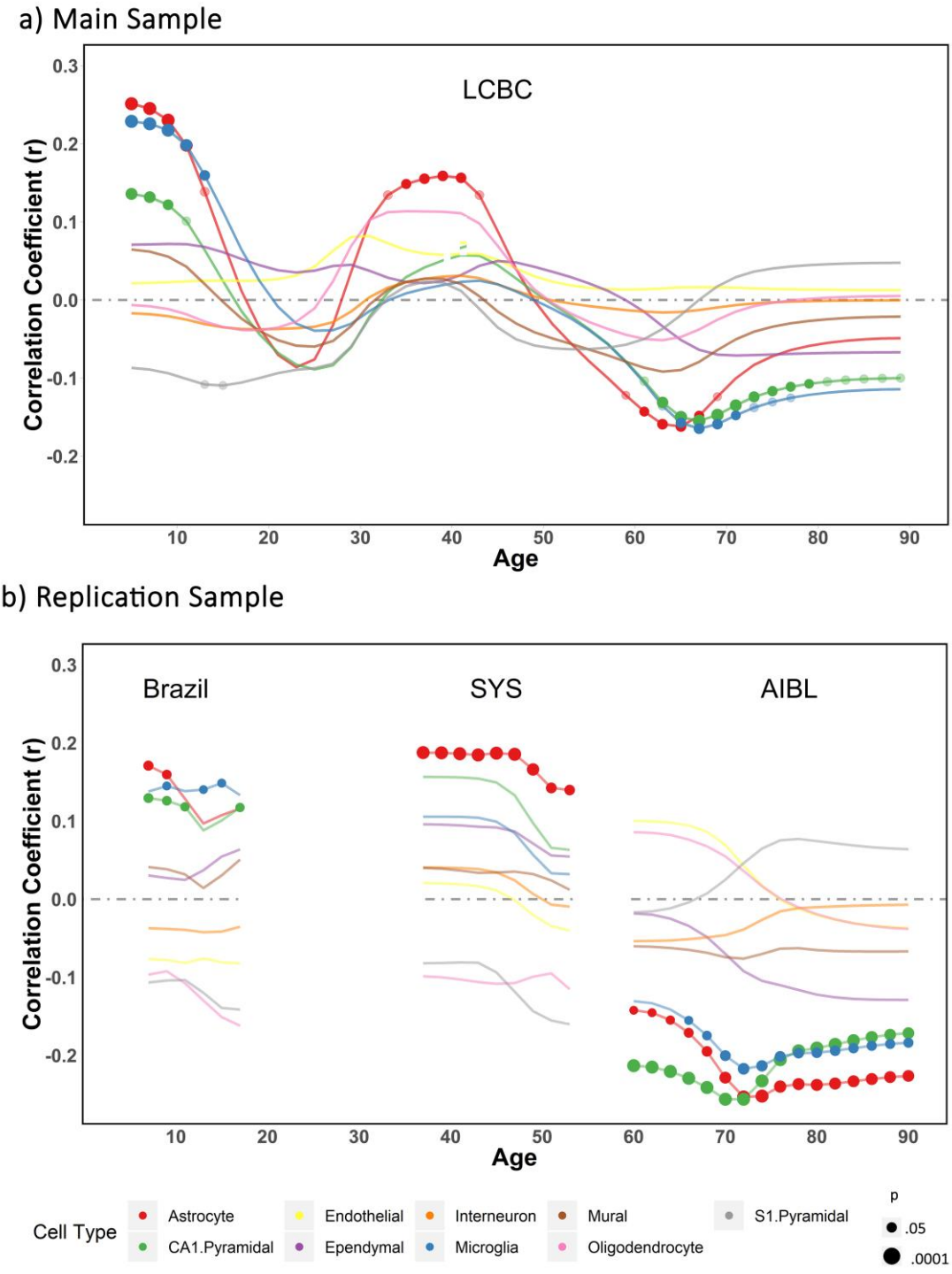

Figure 2. Virtual Histology along the lifespan. *Correlation coefficients between the cortical thinning profile along the lifespan and mean regional profiles of gene expression*

levels in each of the 9 cell types. a) Thinning profile obtained from the LCBC dataset. (n = 4,004 observations). b) Thinning profile for the replication datasets. SYS replication dataset visualization is trimmed after 55 years to avoid overlap with AIBL sample (see SI text for more information). Three different sample cohorts were used corresponding to the age-ranges where significant associations between thinning profile and cell-specific gene expression were found. We used the Brazil High Risk Cohort to encompass school years, the SYS dataset for middle-aged participants, and the AIBL data for older adults (n = 1,174, 548 and, 739 observations, respectively). Significance was tested only for significant thinning – expression correlations in the main sample; thus expression – thinning trajectories of the additional cell-types are included for visual purposes only. For both plots, the x-axis indicates age while the y-axis indicates the correlation of thinning with cell-type specific gene expression as derived from the Allen Human Brain Atlas. Values above 0 represent a relationship of gene expression profiles with reduced thinning - or thickening - while values below 0 represent a relationship with steeper cortical thinning. Circles indicate a significant relationship ($p < 0.05$, permutation inference n = 10,000 iterations) after Bonferroni correction for multiple comparisons along the lifespan (semi-transparent circles) and after additionally applying FDR-adjustment for testing multiple cell-types (opaque circles). The size of the circle represents significance.

Virtual Histology. Cell type – cortical thinning relationship for cell type subclasses.

Next, we tested whether different subclasses of astrocytes, microglia, and CA1 pyramidal cells could account for the cortical thinning – gene expression relationship in the childhood and the aging periods. To facilitate the analysis, we reduced the cortical thinning phenotypes to three developmental periods corresponding to the inter-regional patterns of cortical thinning in childhood (5 – 9 years), middle-age (35 – 41 years) and older age (65 – 67 years). See the cortical thinning profiles in **Fig. 3** and the expression – thinning correlation results in **Fig. 4** and **Table 2**. The results showed that the same cell-type subclasses are associated with thinning profiles during childhood and older adulthood (but – as expected based on the original analysis - with the opposite expression - thinning direction) (**Table 3**).

For CA1 pyramidal cells, only expression for the *CA1Pyr2* subclass was associated with young and old cortical thinning profiles.

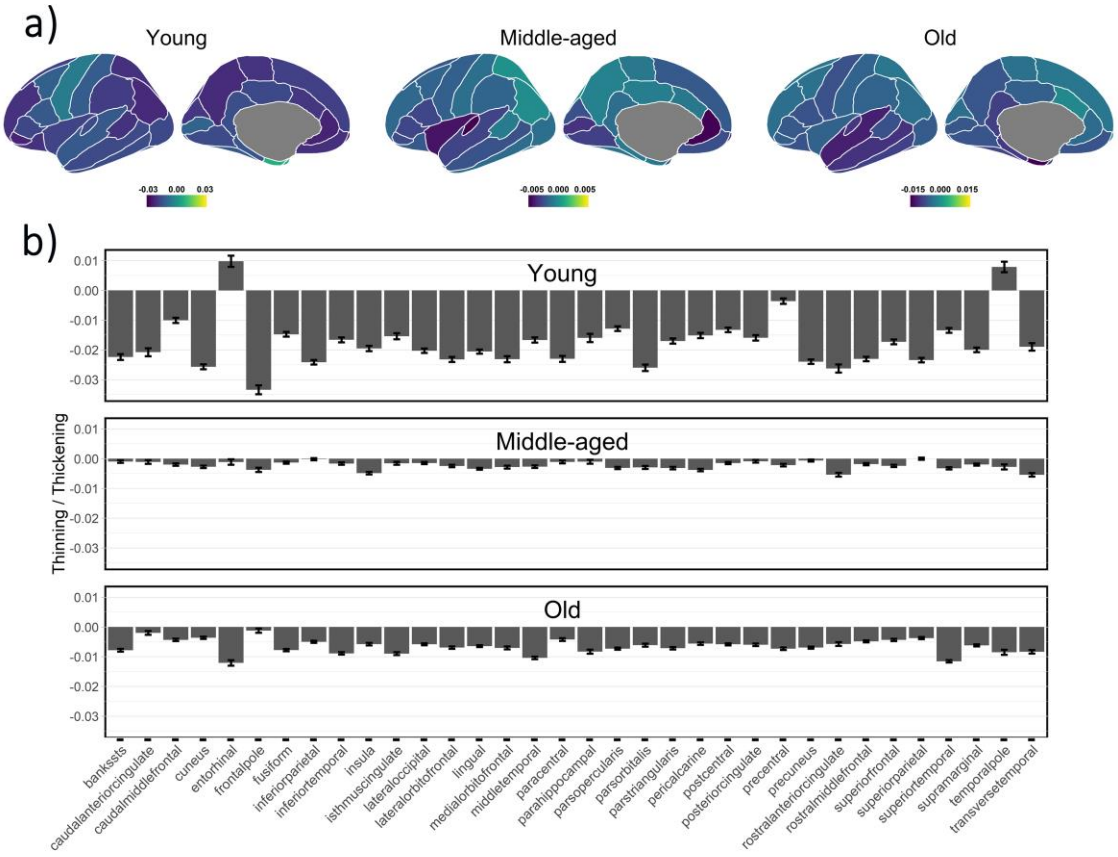

Figure 3. *Inter-regional cortical thinning. Inter-regional patterns of cortical thinning for the age-ranges of interest (i.e. where thinning was significantly related to cell-specific expression). a) Information displayed on a brain representation ("ggseg" R package). b) Information displayed as a graph bar. Error bars represent standard errors of the mean (SEM). The unit of cortical thinning is mm/year.*

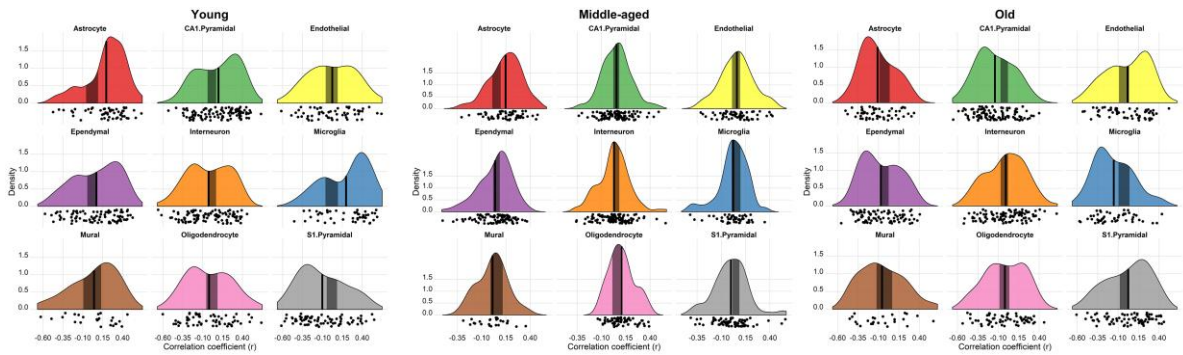

Figure 4. *Expression – thinning correlation. Virtual Histology results at the ages of interest. (i.e., where thinning significantly related to cell-type specific expression). Expression – thinning association at a) childhood (5 – 9 years), b) middle-age (35 -41 years), and c) old age (63-67 years). Each plot shows the distribution of the expression - thinning correlation coefficients for genes in each cell-type group as a density function and as a cloud of dots. The x-axes indicate the coefficients of correlation between the thinning profile and the expression profiles. The y-axes indicate the estimated probability density for the correlation coefficients; the vertical black line indicates the average expression - thinning correlation coefficient across all genes within a cell-type group while the shaded gray box indicates the 95% limits of the empirical null distribution, thus indicating 5% significance level unadjusted between cell-type comparisons. See also* ***Table 2****.*

		Young			Middle-aged			Old		
Cell type	**Genes (n)**	**r**	**p**	**p (fdr)**	**r**	**p**	**p (fdr)**	**r**	**p**	**p (fdr)**
Astrocyte	54	.19	<.001	<.001	.15	<.001	.002	-.11	.005	.02
CA1.Pyramidal	103	.10	.001	.004	.06	.42	.95	-.14	<.001	.001
Endothelial	57	.02	.58	.66	.06	.35	.95	.02	.72	.81
Ependymal	84	.07	.04	.08	.04	.79	1	-.07	.05	.10
Interneuron	100	-.03	.46	.64	.03	.92	1	-.01	.86	.86
Microglia	48	.18	<001	<.001	.02	.90	1	-.15	<.001	.002
Mural	25	.04	.50	.64	.01	.91	1	-.06	.32	.57
Oligodendrocyte	60	-.02	.66	.66	.11	.005	.02	-.02	.66	.81
S1.Pyramidal	73	-.10	.008	.02	.00	1	1.0	.02	.57	.81

Table 2. *Expression – thinning statistics. Main statistics from the expression – thinning correlation analysis at the age of interest (i.e. where thinning significantly related to cell-type specific expression; at young age (5 – 9 years), middle age (35 -41 years), and old age (63-67 years)). Genes indicate the number of genes included in each cell-type group. r indicates the average expression - thinning correlation coefficient across all genes within a cell-type group. "p" and "p-fdr" denote the significance of the average expression - thinning correlation - estimated as a function of the empirical null distribution – before and after FDR-adjustment for n = 9 different cell-type comparisons. See also* ***Fig. 4****.*

			Young			Middle age			Old		
Subclass	**Main class**	**Genes (n)**	**r**	**p**	**rank**	**r**	**p**	**rank**	**r**	**p**	**rank**
Astro1	Astr.	21	.26	**<.001**	2	.18	**<.001**	2	-.16	**.007**	2
Astro2	Astr.	21	.27	**<.001**	1	.22	**<.001**	1	-.15	**.01**	5
CA1Pyr1	CA1.Pyr.	21	.01	.15	12				-.12	.05	7
CA1Pyr2	CA1.Pyr.	21	.21	**.001**	4				-.21	**<.001**	1
CA1PyrInt	CA1.Pyr.	21	.12	.06	9				-.12	.05	6

CA2Pyr2	CA1.Pyr.	21	.06	.34	18	-.06	.29	14.5
Mgl1	Mgl	21	.20	**.002**	5	-.15	**.01**	4
Mgl2	Mgl	21	.16	**.01**	7	-.11	.08	8
Pvm1	Mgl	21	.24	**<.001**	3	-.15	**.008**	3
Pvm2	Mgl	21	.17	**.008**	6	-.08	.20	12

Table 3. *Cell-type subclasses. Relationship between cortical thinning profiles (at young, middle age and old age periods) and gene expression associated with subclasses of astrocytes, microglia, and CA1 pyramidal cells. Rank indicates the ranking of a given cell -type subclass in terms of average expression - thickness correlation coefficients (n = 47 subclasses; ranking in the older period has been reversed). Bold p-values indicate significance after FDR-adjustment for multiple comparisons (n = 10 for young and old and n = 2 for the middle-age thinning profiles). Astr. = Astrocytes, CA1.Pyr = CA1 Pyramidal cells, Mgl = Microglia. Note that in middle-age, only astrocyte subclasses were tested, as, in this period, microglia and CA1 pyramidal-specific gene expression was not associated with cortical thinning (see* ***Fig. 2****).*

Gene Ontology (GO) enrichment analysis. Different processes mediate the cell type – cortical thinning relationship in different age periods.

This analysis was aimed at identifying candidate neurobiological mechanisms that may mediate the cortical thinning - cell-type associations at the different ends of the lifespan. For young and old age, we intersected three different gene ontology (GO) enrichment analyses for biological processes to reveal (1) which were regulated during a particular age period, (2) which were associated with cortical thinning within the same age period, and (3) which were linked to a specific cell type (see **Materials and methods** for details). We found that in young and old age, respectively, 32 and 16 processes were triply enriched (all tests FDR-p < .05); a triply enriched process is one that (1) underwent regulation during young or old age, and (2) was enriched for cortical thinning, and (3) was enriched for a specific cell type (i.e. astrocyte, microglia or CA1-pyramidal neurons). See a visual representation in **Fig. 5** and **Table S1** for a list of triply enriched terms. In younger age, triply enriched processes included “small molecule metabolic”, “catabolic”, “generation of precursor metabolites” and “oxoacid metabolic processes”, which were associated with less regional thinning and the astrocyte cell type, while

"cellular response to stimulus", "vesicle-mediated transport", "cell motility" and "signal transduction" were associated with less regional thinning and the microglia cell type. In older age, triply enriched processes involved "neuron projection morphogenesis", "modulation of chemical synaptic transmission" or "regulation of trans-synaptic signaling", which were associated with steeper cortical thinning and CA1-pyramidal cell-type, while regulation of "cell communication" and "signal transduction", were associated with steeper cortical thinning and the microglia cell-type. In brief, triply enriched processes were centered in astrocytic metabolism in young age, while in older age these were aligned with synaptic communication. Microglial signaling processes were triply enriched both in younger and older age. See detailed GO results in **supporting information.** See Directed Acyclic Graph (DAG) in **Supplementary Fig. 2** for a visual display of biological processes with ongoing regulation during younger (490 processes) and older (95 processes) age.

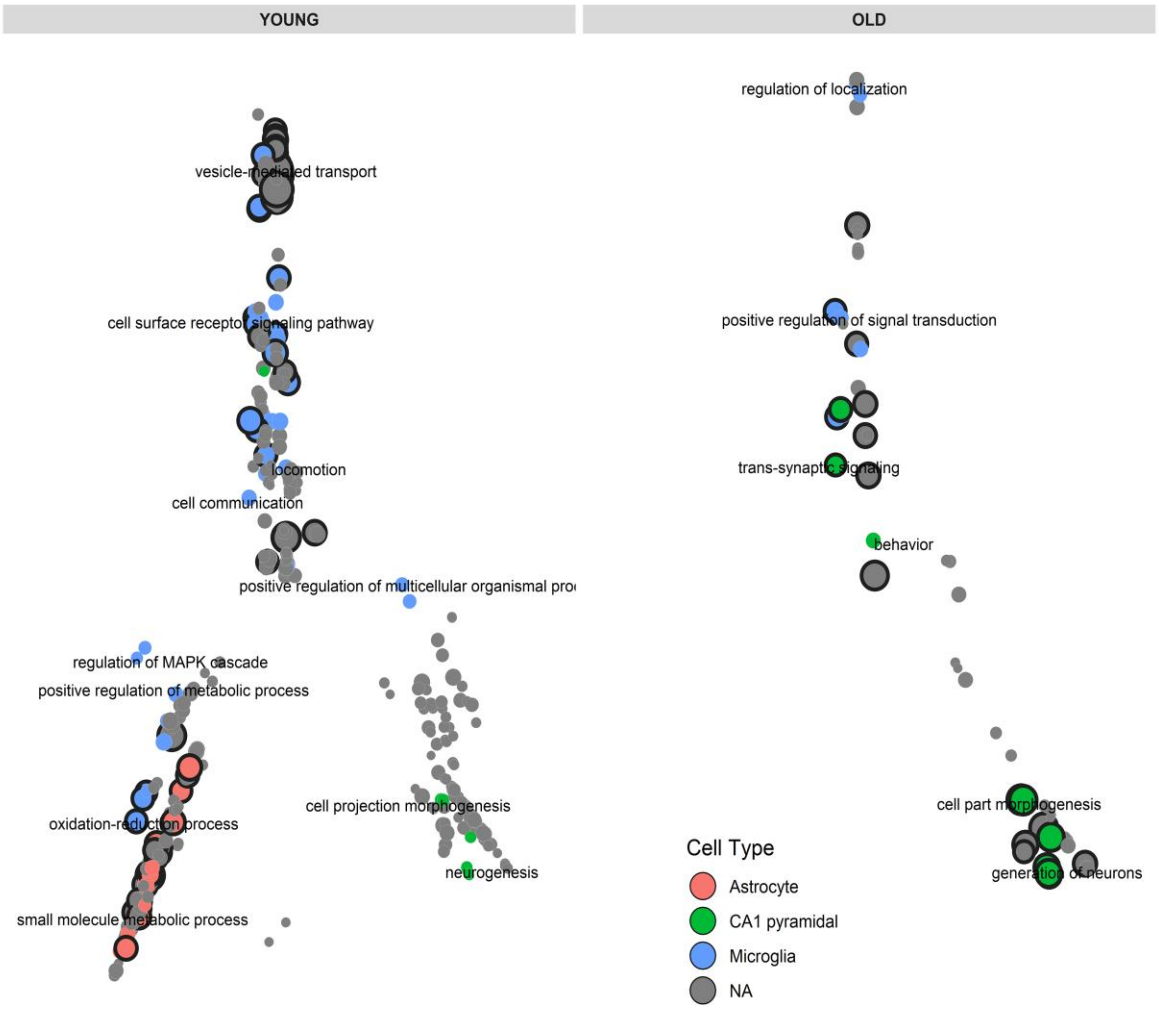

Figure 5. *GO intersection. Circles represent biological processes associated with changes in gene expression during an age period (i.e. young or older age). Black borders additionally display those GO gene sets enriched for genes associated with cortical thinning. Blue (microglia), green (CA1 pyramidal) and, red (astrocytes) represent biological processes enriched for cell-specific genes. Significance is considered at p < 0.05 FDR-corrected in all the enrichment analyses. Biological processes are spread along the X and Y-axis based on Lin's Semantic Similarity as implemented in the "GOSemSim" R-package* [81]*. See also* ***Table S1****.*

Discussion

In this study, we showed that inter-regional profiles of cortical thinning estimated from MRI relate to expression profiles for marker genes of CA1 pyramidal cells, astrocytes and microglia. The relationships were particularly evident during development and aging but in opposite directions. Across the 34 cortical regions, higher expression of cell-specific genes was associated with less thinning in younger age and steeper thinning in older age. Additional enrichment analyses suggest that cell type – thinning relationships might rely on partially different mechanisms in younger and older age. The implications of the results are discussed below.

Remarkably, we found that cell-type expression - thinning patterns during development are mirrored later in life. The interregional profiles of cortical thickness also exhibit the same pattern as over 70% of the variance of the thickness profile is explained by astrocytes, microglia, and CA1-pyramidal-specific gene expression [28]. This overarching pattern fits with the view that thinning during developmental and old age periods closely resemble a topography based on common genetic influences [7]. While the same cell types are involved in cortical thinning at different periods in life, it is unclear whether the same or different molecular functions are at play. As cortical thinning and thus the expression - thinning correlations change over the lifespan, the cell-type associations can be understood at least from three different angles: 1) cortical thinning reflects a direct loss of cell numbers or – more likely – volume 2) cell-specific processes – e.g., apoptosis, metabolic demands – mediate indirectly the relationship between cell-type and thinning of the cerebral cortex, 3) an interaction between developmental (or neurodegenerative) processes and MRI acquisition parameters or analytical features – e.g. shifts in T1/T2 boundary may occur due to myelination [11].

The association of astrocytes, microglia and CA1 pyramidal cells with less cortical thinning during development replicates our earlier findings in an independent, cross-sectional sample [28]. Involvement of CA1-pyramidal cells with less cortical thinning agrees with the notion that axonal sprouting and remodeling of dendritic arbor are associated with relative thickening of the developing cerebral cortex [7]. CA1 pyramidal genes are highly enriched for terms such as "regulation of dendrite extension" in contrast with S1 pyramidal genes, enriched by terms associated with potassium transport and activity [28]. A plausible theory is that the thinning profiles in childhood and early adolescence are primarily dependent on the regional dynamics of dendritic growth. At mid-adolescence, the CA1 expression – thinning relationship disappears. It is possible that intra-cortical myelination or a shift in dendritic dynamics might dominate the profile of inter-regional variation in cortical thinning in late adolescence (see further discussion of myelination processes in the technical considerations section) [16,27].

In aging, regions with high CA1 pyramidal expression coincide with those undergoing steeper thinning. This observation fits with both existing histological evidence and current predictions that link dendritic shrinkage with reduced cortical thickness in older brains [17–19,32]. Although neuronal numbers seem preserved in aging [23,33], recent evidence suggests that specific neural subpopulations numbers – namely neurons with large cell bodies – might decrease in aged brains [34]. Again, S1 pyramidal expression was unrelated to thinning with advancing age, which is consistent with evidence that neuron-specific changes of gene expression with age are dependent on cellular identity [34,35]. A promising direction requires linking variations of neuronal properties –including regional variations in dendritic and soma size - with MRI estimates of cortical thinning [36]. As a proof of principle, we found that for CA1 pyramidal cells, only expression for the *CA1Pyr2* subclass was associated with the thinning profiles. Expression of *CA1Pyr2*-specific genes is associated with mitochondrial function, which correlates with the firing rate and length of projections in cortical neurons [31].

Expression of genes specific to astrocytes and microglia was associated with cortical thinning in both younger and older ages. These two cell types represent around 19% and 6% of the glial cells in the neocortex [23], and these numbers are preserved or - for microglia – even increased during the lifespan [23,37–39]. Thus – despite modest changes in the cell morphology throughout the lifespan [37,40] - it is more likely that the relationship between cortical thinning and these glial subpopulations relates to interactions with other neural components. This interpretation agrees with the notion that both astrocytes and microglia functions are highly adaptable and dependent on the biological environment and that their response profile changes with age. It is also consistent with the observations that both microglia and astrocyte genes are up-regulated homogenously in the cerebral cortex with advancing age [34,35], which leans towards a reactive phenotype for astrocytes and a shift to a pro-inflammatory profile for microglia [41,42].

As astrocytes and microglia have multiple biological functions in the human brain and it is unclear which of these functions are related to cortical thinning and whether the relationship is stable across different age periods. One can anchor the expression – thinning associations to age-specific neurobiological mechanisms by identifying those processes that undergo regulation during a given age period. The assumption is that genes that change in expression will link to critical processes taking place at a given period in life. We found several metabolic processes to be triply enriched in younger age. This means that they undergo expression changes during development, relate to the childhood cortical thinning profile and are astrocyte-specific. Astrocytic metabolic processes – mainly of glycolytic nature – provide energy substrates to the brain [43]. In the human brain, metabolic requirements peak in childhood and until puberty [44]. Astrocytes distribute energy substrates – mostly lactate – to active neurons [45,46], sustaining glutamatergic neurotransmission, synaptic plasticity, and thus long-term memory formation [47]. Genes associated with metabolic processes remained unaltered

in aging, in congruence with Boisvert et al. [48] who found that astrocytic homeostatic genes were largely unchanged with aging.

The GO analyses pointed out diverse signaling pathways as candidates to mediate the microglia – thinning relationship in both young and old age. These results highlight the versatility and the responsiveness of microglia to the surrounding environment [49]. As microglia are very sensitive to changes in the surrounding environment [50], they might exert different functions with opposite effects depending on the period of life. Microglia engage in crosstalk with neurons and astrocytes, and can modulate synaptic homeostasis and remodel synaptic structures. Substantial changes characterize the aging microglia, both in morphology and function [41,49]. It is unclear which microglial processes are involved in cortical thinning in aging, but one speculation is that it has a role in the removal of myelin and cellular debris, which seems to contribute to the wear and tear of microglia in the aging brain [51].

Technical considerations

Two features of the study require special consideration, namely the source of variability and the correlational nature of the analyses. The main measure of the study is the interregional profile of cortical thinning (at different ages). While it represents a robust and stable measure, the interregional thinning profile is unable to provide information neither at an individual level nor across time; hence, a portion of the variability remains unexplored. Relative disparity amongst studies might reside on different characterizations of cortical thinning variability [27]. Correlational tests are unavoidable when exploring the underlying mechanisms of cortical thinning *in vivo*, yet longitudinal comparisons (i.e. individual rates of thinning) will approximate better the dynamic relationship of thinning and its neurobiological foundations across the lifespan.

Certain questions remain open and require further research, such as the role of oligodendrocytes on adolescent cortical thinning as intra-cortical myelination should correlate with steeper thinning. In particular, MRI estimates of myelin content have been associated both with steeper cortical thinning in adolescents and cortical thickness as measured with MRI [11,26,27,52]. Lack of findings may relate to the nature of the interregional profiles, which represent snapshots in time and, hence, are determined by the differential sum of processes that modulate cortical thickness in each area. Thus, it is plausible that the lack of results in regards to oligodendrocytes relate to the dimension in which we observed the variability (i.e. interregional profile vs. regional developmental trajectories). Nonetheless, we observed an (uncorrected) relationship of S1-pyramidal cells and oligodendrocytes (in the replication sample) expression profiles and steeper thinning in late adolescence. This observation might indicate the cortical thinning profile becomes dominated by myelination processes in later phases of brain maturation and with the notion that morphological features of pyramidal cells, such as dendritic tree size or branching, have dissimilar regional trajectories throughout development [53]. Altogether, it is likely that, at least in early phases of life, diverging mechanisms promote at the same time thinning and thickening of the cerebral cortex [32].

Conclusion

Considerable work has been devoted to the understanding of the relationship between microscale neuronal features and macroscopic morphology [36,54–56]. Yet, the underlying mechanisms driving macroscopic cortical changes remain largely unknown. Thus, understanding the biological substrate underlying MRI-based estimates of cortical thinning during different stages of the lifespan remains a key issue in neuroscience given the ever-increasing use of neuroimaging and the association of cortical thickness variations with neurodevelopmental and neurodegenerative pathology. We found that cortical thinning was associated with CA1 pyramidal cell, astrocytes, and microglia expression in

development and that this was mirrored in aging with reverse relations. These results were replicated in independent MRI datasets. The processes underlying these associations seem to differ at both ends of the lifespan. Astrocytic metabolic processes appear prominently related to regional variations in cortical thinning earlier in life while synaptic changes and alterations in pyramidal morphology appear to be dominantly involved in the thinning profile in aging. Microglia's relationship with cortical thinning in both lifespan periods appears to articulate through signaling pathways. These findings represent a contribution towards understanding the neurobiological mechanisms underlying cortical thinning across the lifespan.

Material and methods

MRI sample

A total of 4,004 scans from 1,899 healthy participants (1,135 females) ranged between 4.1 – 89.4 years of age (mean visit age = 37.4 [SD = 25.3]) were drawn from six Norwegian studies coordinated by the Center for LCBC: The Norwegian Mother and Child Cohort Neurocognitive Study [57]; Neurocognitive Development [58]; Cognition and Plasticity Through the Lifespan [59]; Constructive Memory [60]; Method of Loci [61]; and Neurocognitive plasticity [62]. More than one scan was available for 1,017 participants; the mean number of scans per participant was 2.1 (range 1-6) spanning up to 11.1 years after the initial scan. The density of sampling was higher in the childhood/adolescence and during the 7th and 8th decade of life. See **Supplementary Fig. 3** and **Table 1** for a visual representation and descriptive information.

In all studies, participants were screened through health and neuropsychological assessments. Common exclusion criteria consisted of evidence of neurologic or psychiatric disorders, learning disabilities or current use of medicines known to affect the nervous system. In addition, participants were excluded from the current study based on the following criteria: lack of a valid structural scan (i.e. excessive movement, acquisition or surface reconstruction errors), score <25 on the Mini Mental State Examination (MMSE) [63], score of ≥20 on the Beck Depression Inventory (BDI) [64], and age > 90 due to low sampling density after this age. All the studies were approved by a Norwegian Regional Committee for Medical and Health Research Ethics. See **SI text** for further details on samples.

For replication, we used three additional samples that encompassed the age periods in which we observed associations between regional patterns of cortical thinning and cell-specific gene expression. We used the Brazil High Risk Cohort [65] to replicate findings during childhood/adolescence. For replication of results in middle-age, we used the cohort of parents of the Saguenay Youth Study (SYS) [66]. For older adults, the replication sample was collected by the AIBL study group. AIBL study methodology has been reported previously [67]. See **Supplementary Fig. 3, Supplementary Table 3** and **SI text** for the replication sample description.

MRI acquisition and preprocessing

LCBC image data were collected using four different scanners. Three scanners (*Avanto2 [1.5 T], Prisma [3.0 T] and Skyra [3.0 T];* Siemens Medical Solution) were located at Oslo University Hospital Rikshospitalet while the remaining (*Avanto1 [1.5 T])* was placed at St. Olav's University Hospital in Trondheim. For 285 participants, data were available for two or more MRI machines from the same day (n = 285). For each participant and visit, we obtained a T1-weighted magnetization prepared rapid gradient echo (MPRAGE) sequence. See **SI text** for MRI acquisition parameters in both the LCBC and the replication datasets.

Data were processed on the Colossus processing cluster, University of Oslo. We used the longitudinal FreeSurfer v.6.0. stream [68] for cortical reconstruction of the structural T1-weighted data (http://surfer.nmr.mgh.harvard.edu/fswiki) [69–71]. See the pipeline description in **SI text**. See **SI text** for differences in the MRI processing pipeline in the replication datasets.

MRI analysis. Estimation of cortical thinning along the lifespan.

After the surface reconstruction, MRI-based estimates of cortical thickness were extracted for the 34 left hemisphere ROIs corresponding to the Desikan-Killiany atlas [29]. We ran an analysis to estimate each region's cortical thinning - or thickening - at any given point during the lifespan. The MRI analysis was implemented in R (www.r-project.org).

First, for each of the 34 cortical regions, thickness data were fitted to age using generalized additive mixed models (GAMM) with "mgcv" R package [72]. The GAMM fitting technique represents a flexible routine that allows nonparametric fitting with relaxed assumptions about the relationship between thickness and age [7]. The technique is well suited for fitting nonlinear relationships through local smoothing effects, independent of any predefined model, and robust to age-range selections and distant data points [73].

All GAMM models included sex and scanner as covariates and participant identifiers as random effects. We specified cubic splines as smooth terms [72] and limited to k = 6 the knots of the spline, a somewhat conservative option to minimize the risk of overfitting and to increase the stability of the derivatives. See **SI text** for results with a varying number of knots. Next, we excluded those observations ± 7 SD above or below the cortical thickness trajectory (mean = 3.2 [1.8 SD] observations excluded per region). After outlier removal, cortical thickness data were re-fitted by age with GAMM (separately in each region).

Finally, we considered the GAMM derivatives to obtain the trajectories of cortical thinning along the lifespan. For each region, we obtained the derivative – and its confidence intervals - based on a finite differences approach as implemented in the "*schoenenberg"* R package (https://github.com/gavinsimpson/schoenberg). Positive values in the derivative are interpreted as higher cortical thickening while negative values are interpreted as steeper thinning at any given age. For each cortical region, we then extracted the derivative values at discrete ages (from 5 to 89 years; every 2 years) resulting in n = 43 cortical thinning profiles spanning from childhood to old adulthood.

We created an interactive platform using the "shiny" R package to allow the exploration of both the trajectories of cortical thickness and thinning along the lifespan, and the inter-regional profiles of cortical thinning at any age (**supporting information**). Also for visualization, we computed the estimated trajectories of cortical thickness and thinning during the lifespan using weighted average cortical thickness – across the 34 ROIs – as the fitting data.

Gene expression analysis. Estimation of cell-specific gene expression across the cortical surface.

We used the scripts provided by French et al. [28] to obtain gene expression profiles across the left hemisphere. All the in-house procedures were implemented in R (www.r-project.org). Note that only genes with inter-regional profiles consistent across the six donors (Allen Human Brain Atlas) and across two datasets (Allen Human Brain Atlas and the BrainSpan Atlas) were used (see below for details).

Gene expression profile

Gene expression data were obtained from the Allen Human Brain Atlas, based on postmortem human brains, providing comprehensive coverage of the normal adult brain (http://www.brain-map.org) [30]. Isolated RNA was hybridized to custom 64K Agilent microarrays (58,692 probes) by the Allen Institute. Gene expression data for the left hemisphere were available for six donors (five males aged 24, 31, 39, 55 and 57 years; and one female aged 49 years).

As previously described [74], gene-expression data from the Allen Human Brain Atlas were mapped to the Desikan-Killiany atlas in FreeSurfer space yielding up to 1,269 labeled samples per brain inside or close to a FreeSurfer cortical region [29]. The expression values of the mapped samples were mean averaged across microarray probes to provide a single expression value for each gene for a given sample. Median averages were used to summarize expression values within each of the ROI and donor, which was followed by the median average across the six donors. This yielded a single value for each region representing the median profile for a given gene across the 34 cortical regions.

Consistency of inter-regional profiles in gene expression

The consistency of the inter-regional gene expression profiles was assessed with a two-stage procedure after which we retained a panel of (n = 2,511) genes with consistent gene expression profiles from the original 20,737 genes profiled in the Allen Human Brain Atlas.

In stage 1, we calculated the mean Spearman correlation between each of the six donor's profiles and the median (group) profile for each gene. Using this metric, the median profile provides a good approximation across the donors for 39.7% of the assayed genes (rho > 0.446 corresponding to one-sided $p < 0.05$ derived from random simulations of donor expression profiles) [74]. In stage 2, we relied on the BrainSpan Atlas, which provides gene expression data in the developing human brain (www.brainspan.org) [75] as previously implemented [28]. We limited the samples to age > 12 years (n = 9

donors) and downloaded gene expression values obtained in 11 cortical regions included in the BrainSpan atlas that are homologous to those on the Desikan-Killiany parcellation employed in the Allen Human Brain Atlas. Next, we compared the similarity between the regional profile between the Allen Human Brain Atlas and the BrainSpan Atlas across the 11 cortical regions available in both atlases. Only genes that showed a correlation between the two profiles higher than $r = 0.52$ (one-sided test $P < 0.05$) were retained.

Panels of Cell-Specific Marker Genes

Lists of genes expressed in specific cell types were obtained from Zeisel et al. [31]. In their study, single-cell transcriptomes were obtained for 3,005 cells from the somatosensory cortex (S1) and the CA1 hippocampus region of mice. Gene expression was then biclustered into nine classes that contained each over 100 genes.

We converted mouse genes to human gene symbols using the HomoloGene database (http://www.ncbi.nlm.gov/homologene) [76], as implemented in the *"homologene"* R package (https://github.com/oganm/homologene). The resulting classes of cell types and the number of marker genes kept after consistent genes were filtered are: S1 pyramidal neurons (n = 73 human gene symbols), CA1 pyramidal neurons (n = 103), interneurons (n = 100), astrocytes (n = 54), microglia (n = 48), oligodendrocytes (n = 60), ependymal (n = 84), endothelial (n = 57), and mural (pericytes and vascular smooth muscle cells; n = 25).

Panels of Subclass Cell-Specific Marker Genes

In addition to the main nine classes of cells described above, we explored the association between cortical thinning and expression for specific subclasses of cells. Expression of genes associated with a

specific subtype of cell was obtained from Zeisel et al. [31]. In their study, each cell (n = 3,005) was classified both into a main and a second-level type of cell based on the expression profile. Most of the subclasses have anonymous tags but do also include some known markers, layer or region information. Following previous work [35], each gene was converted to human gene symbols. We log-transformed the RPKM values, added 1 and, Z-standardized the values across cells. Genes with average standardized expression levels higher than two standard deviations in a given transcriptomic cell type were considered cell-type enriched. Cell subclass panels of genes were obtained by filtering the n = 2,511 genes (with consistent inter-regional profile) and restricting each subclass panel up to 21 marker genes.

Gene Ontology Enrichment Analyses. Gene lists.

We carried out a series of Genetic Ontology (GO) Enrichment Analyses to further understand the role of specific cell-types on cortical thinning in each age period of interest, namely in younger and older ages. Specifically, we intersected three different GO enrichment analyses to reveal which biological processes were regulated during an age period, were associated with cortical thinning - in the same age period - and could be linked to a specific cell type. The list of genes whose expression was associated with age-specific up/down regulation, cortical thinning and, specific cell-types was obtained as explained below.

List of genes associated with expression regulation at critical age periods

First, we obtained two lists of genes that were linked with expression regulation in young and old age. To do so, we used post-mortem gene expression values of the human cortex from the following

expression sources: BrainCloud [77], Brain eQTL Almanac (BrainEAC) [78], BrainSpan [75], and Genotype Tissue Expression (GTEx) [79]. 1,013 tissue samples from donors aged between 0 and 92 years were considered (mean age = 44.9 [SD = 22.3]; 158 females; 1-11 regions). See details of each dataset in the supplementary information and demographics of each source in **Table S2**. Only genes with expression in all datasets were considered. For each gene and dataset, gene expression values were scaled and fed into a GAMM analysis (smooth term = cubic spline; knots = 8) that included age as the smooth term, sex as covariates, and dataset and donor identifiers as random effects. 1.0% of the genes were discarded due to fitting problems (mostly convergence issues). After computing the derivative of the fittings - as detailed above – we considered genes undergoing up/down-regulation those whose derivative deviated > 3 SEM during the young and old age periods. Of the 15,693 fitted genes (background genes), 3,807 and 3,508 were being up and down-regulated during the young period and 569 and 661 during the old period.

List of genes associated with cortical thinning critical age periods

We obtained a list of genes associated with inter-regional variations of cortical thinning at younger and older age. The cortical thinning list included the top 10% of genes (n = 2 074) associated with less cortical thinning at younger age and more cortical thinning at older age (due to specific directionality of the cell type – cortical thinning relationship). The expression – thinning relationship was $r > .38$ and $r < -.32$ for the young and old lists ($p < .013$ and $p < .03$, one-tailed, n = 34 regions). The background list included 20,737 genes with expression – thinning values. Note that no consistency filter was applied as GO terms were associated with consistency [74] and to increase the power of the analysis.

List of genes associated with specific cell-types

We obtained a list of genes associated with astrocyte, microglia and CA1-pyramidal cell types. The background list consisted on the n = 2,767 cell-specific genes reported in [31] while as foreground we used those specific to CA1-pyramidal (n = 357), astrocytes (n = 214) and, microglia (n = 374).

Higher-level statistical analysis

Correlation between lifespan thinning and cell-specific gene expression profiles

In the main analysis, we assessed the relationship between the inter-regional profiles of cortical thinning – obtained from the GAMM derivative sampled between 5 and 89 years - and the inter-regional profiles of gene expression associated with specific cell types. For each cortical profile and marker gene, we computed the Pearson correlation coefficients between the thinning profile and the median inter-regional profile of gene expression levels for each marker gene; yielding a gene-specific measure of expression - thinning correlation.

We used a resampling-based approach to test the association between cell-type expression and cortical thinning profiles [28]. The average expression - thinning correlation for each group of cell-specific genes served as the test statistic (i.e. mean correlation between cortical phenotype and cell-specific gene expression). In addition, we controlled for multiple comparisons, accounting both for the number of cortical thinning profiles (i.e. age points n = 43) and for the different cell-types (n = 9).

For each cell-type panel, we obtained the empirical null distribution of the test statistic as follows. 1) From all the (n = 2,511) consistent genes, we randomly selected the same number of genes as that of the genes in the cell-type group under consideration. 2) For each thinning profile (n = 43 sampled ages), we averaged the expression - thinning correlation coefficients of all the selected genes. Thus,

for each random sample, we obtained the mean correlation coefficients at each age. (3) Of the n = 43 coefficients, we selected the one with absolute maximum expression - thinning correlation. This step is essential to introduce a Bonferroni-like correction for multiple comparisons at a within cell-type level while accounting for the non-independency of the thinning estimates (e.g. the cortical thinning profiles at age 60 and 62 are not independent observations). The null distribution was estimated by repeating the previous three steps for 10,000 iterations. A two-sided p-value was computed as the proportion of average thinning – expression correlations whose values exceeded the average for the genes in the original cell-type group. We rejected the null hypothesis at p = .05 False Discovery Rate (FDR)-adjusted significance thus correcting for multiple testing of the nine cell-type groups.

The same procedure was run for the three replication-samples with the following variations. The number of within cell-type comparisons was defined by the specific age range of each replication sample (n = 6, 15 and 17 2-year steps for Brazil, SYS, and AIBL datasets, respectively). Second, significance testing and FDR between cell-type corrections were only applied for those cell-type groups that were significant in the main analysis.

Post-hoc analysis. Correlation with cell-type subclasses

We explored further whether specific subclasses of astrocytes, microglia, and CA1-pyramidal cells – the three cell types whose expression related to the thinning profiles at different age periods (see below) - were associated differently with cortical thinning profiles at the different developmental periods. For each developmental period of interest – namely, childhood, middle-age and older age - the cortical profiles of thinning were averaged to a single phenotype per period. Then, we assessed the correlation between thinning profiles in childhood, middle-aged and old adulthood and gene expression profiles for each subtype of cell as described before – excluding the multiple comparisons correction for age. In addition, the different subclasses of interest were ranked - i.e. from higher to

lower expression - thinning correlation - to better evaluate whether different cell-type subclasses drive the thinning-expression relationship in the childhood and the aging periods. The results were plotted with "ggplot2" R package tools to ease inspection of data.

Gene Ontology Enrichment Analysis. Term intersection

To study those biological processes that are associated with specific cell-types, cortical thinning and age-related regulation in both young and old age, we carried out three different GO enrichment analyses and intersected the results. GO term enrichment was performed with VisuaL Annotation Display (VLAD; version 1.6.0) [80] using the Human Gene-function annotation from Gene Ontology Annotation (GOA) Database. Only the Biological Process ontology was considered.

First, we obtained those terms associated with age-dependent regulation (i.e. associated with genes that are being up/down-regulated in young and old age; FDR-p < .05). Both lists of up and down-regulated genes were simultaneously fed to the term enrichment software. We considered the resulting terms (n = 440 and 95 for young and old age periods) as biological processes that were regulated during younger and older age and thus likely candidates to drive age-specific patterns of cortical thinning. Term enrichment for cortical thinning (at each age) and cell-type (CA1, astrocytes, and microglia) was then performed in the surviving biological processes (FDR p < .05 corrected). Biological processes enriched for cell-type and cortical thinning and, importantly, regulated during a given age period represent likely mechanisms for cell type-dependent cortical thinning of the brain. Enriched terms were plotted as a function of Lin's semantic similarity – as implemented in the "GOSemSim" R-package [81].

References

1. Walhovd, K. B. *et al.* Long-term influence of normal variation in neonatal characteristics on human brain development. *Proc. Natl. Acad. Sci. U.S.A.* **109**, 20089–20094 (2012).
2. Grydeland, H., Westlye, L. T., Walhovd, K. B. & Fjell, A. M. Intracortical Posterior Cingulate Myelin Content Relates to Error Processing: Results from T1- and T2-Weighted MRI Myelin Mapping and Electrophysiology in Healthy Adults. *Cereb. Cortex* (2015). doi:10.1093/cercor/bhv065
3. Miller, K. L. *et al.* Multimodal population brain imaging in the UK Biobank prospective epidemiological study. *Nat. Neurosci.* **19**, 1523–1536 (2016).
4. Grasby, K. L. *et al.* The genetic architecture of the human cerebral cortex. *bioRxiv* 399402 (2018). doi:10.1101/399402
5. Hofer, E. *et al.* Genetic Determinants of Cortical Structure (Thickness, Surface Area and Volumes) among Disease Free Adults in the CHARGE Consortium. *bioRxiv* 409649 (2018). doi:10.1101/409649
6. Shin, J. *et al.* Planar cell polarity pathway and development of the human visual cortex. *bioRxiv* 404558 (2018). doi:10.1101/404558
7. Fjell, A. M. *et al.* Development and aging of cortical thickness correspond to genetic organization patterns. *Proc. Natl. Acad. Sci. U.S.A.* **112**, 15462–15467 (2015).
8. Paus, T. Imaging microstructure in the living human brain: A viewpoint. *Neuroimage* **182**, 3–7 (2018).
9. Fjell, A. M. *et al.* One-year brain atrophy evident in healthy aging. *J. Neurosci.* **29**, 15223–15231 (2009).
10. Potvin, O., Dieumegarde, L., Duchesne, S. & Alzheimer's Disease Neuroimaging Initiative. Normative morphometric data for cerebral cortical areas over the lifetime of the adult human brain. *Neuroimage* **156**, 315–339 (2017).

11. Walhovd, K. B., Fjell, A. M., Giedd, J., Dale, A. M. & Brown, T. T. Through Thick and Thin: a Need to Reconcile Contradictory Results on Trajectories in Human Cortical Development. *Cereb. Cortex* **27**, 1472–1481 (2017).
12. Huttenlocher, P. R. Synaptic density in human frontal cortex - developmental changes and effects of aging. *Brain Res.* **163**, 195–205 (1979).
13. Huttenlocher, P. R. & Dabholkar, A. S. Regional differences in synaptogenesis in human cerebral cortex. *J. Comp. Neurol.* **387**, 167–178 (1997).
14. Sowell, E. R. *et al.* Longitudinal mapping of cortical thickness and brain growth in normal children. *J. Neurosci.* **24**, 8223–8231 (2004).
15. Paus, T., Keshavan, M. & Giedd, J. N. Why do many psychiatric disorders emerge during adolescence? *Nat. Rev. Neurosci.* **9**, 947–957 (2008).
16. Patel, Y. *et al.* Maturation of the Human Cerebral Cortex During Adolescence: Myelin or Dendritic Arbor? *Cereb. Cortex* (2018). doi:10.1093/cercor/bhy204
17. Peters, A. & Sethares, C. The effects of age on the cells in layer 1 of primate cerebral cortex. *Cereb. Cortex* **12**, 27–36 (2002).
18. Lu, T. *et al.* Gene regulation and DNA damage in the ageing human brain. *Nature* **429**, 883–891 (2004).
19. Esiri, M. M. Ageing and the brain. *J. Pathol.* **211**, 181–187 (2007).
20. Shaw, P. *et al.* Intellectual ability and cortical development in children and adolescents. *Nature* **440**, 676–679 (2006).
21. Schnack, H. G. *et al.* Changes in Thickness and Surface Area of the Human Cortex and Their Relationship with Intelligence. *Cereb Cortex* **25**, 1608–1617 (2015).
22. Sloper, J. J., Hiorns, R. W. & Powell, T. P. A qualitative and quantitative electron microscopic study of the neurons in the primate motor and somatic sensory cortices. *Philos. Trans. R. Soc. Lond., B, Biol. Sci.* **285**, 141–171 (1979).

23. Pelvig, D. P., Pakkenberg, H., Stark, A. K. & Pakkenberg, B. Neocortical glial cell numbers in human brains. *Neurobiol. Aging* **29**, 1754–1762 (2008).

24. Druga, R. Neocortical inhibitory system. *Folia Biol. (Praha)* **55**, 201–217 (2009).

25. Carlo, C. N. & Stevens, C. F. Structural uniformity of neocortex, revisited. *Proc. Natl. Acad. Sci. U.S.A.* **110**, 1488–1493 (2013).

26. Natu, V. S. *et al.* Apparent thinning of visual cortex during childhood is associated with myelination, not pruning. *bioRxiv* 368274 (2018). doi:10.1101/368274

27. Whitaker, K. J. *et al.* Adolescence is associated with genomically patterned consolidation of the hubs of the human brain connectome. *Proc. Natl. Acad. Sci. U.S.A.* **113**, 9105–9110 (2016).

28. Shin, J. *et al.* Cell-Specific Gene-Expression Profiles and Cortical Thickness in the Human Brain. *Cereb. Cortex* **28**, 3267–3277 (2018).

29. Desikan, R. S. *et al.* An automated labeling system for subdividing the human cerebral cortex on MRI scans into gyral based regions of interest. *Neuroimage* **31**, 968–980 (2006).

30. Hawrylycz, M. J. *et al.* An anatomically comprehensive atlas of the adult human brain transcriptome. *Nature* **489**, 391–399 (2012).

31. Zeisel, A. *et al.* Brain structure. Cell types in the mouse cortex and hippocampus revealed by single-cell RNA-seq. *Science* **347**, 1138–1142 (2015).

32. Fjell, A. M. & Walhovd, K. B. Structural brain changes in aging: courses, causes and cognitive consequences. *Rev Neurosci* **21**, 187–221 (2010).

33. Pakkenberg, B. *et al.* Aging and the human neocortex. *Exp. Gerontol.* **38**, 95–99 (2003).

34. Soreq, L. *et al.* Major Shifts in Glial Regional Identity Are a Transcriptional Hallmark of Human Brain Aging. *Cell Rep* **18**, 557–570 (2017).

35. French, L., Ma, T., Oh, H., Tseng, G. C. & Sibille, E. Age-Related Gene Expression in the Frontal Cortex Suggests Synaptic Function Changes in Specific Inhibitory Neuron Subtypes. *Front Aging Neurosci* **9**, 162 (2017).

36. Scholtens, L. H., Schmidt, R., de Reus, M. A. & van den Heuvel, M. P. Linking macroscale graph analytical organization to microscale neuroarchitectonics in the macaque connectome. *J. Neurosci.* **34**, 12192–12205 (2014).

37. VanGuilder, H. D. *et al.* Concurrent hippocampal induction of MHC II pathway components and glial activation with advanced aging is not correlated with cognitive impairment. *J Neuroinflammation* **8**, 138 (2011).

38. Tremblay, M.-È., Zettel, M. L., Ison, J. R., Allen, P. D. & Majewska, A. K. Effects of aging and sensory loss on glial cells in mouse visual and auditory cortices. *Glia* **60**, 541–558 (2012).

39. Robillard, K. N., Lee, K. M., Chiu, K. B. & MacLean, A. G. Glial cell morphological and density changes through the lifespan of rhesus macaques. *Brain Behav. Immun.* **55**, 60–69 (2016).

40. Jyothi, H. J. *et al.* Aging causes morphological alterations in astrocytes and microglia in human substantia nigra pars compacta. *Neurobiol. Aging* **36**, 3321–3333 (2015).

41. Olah, M. *et al.* A transcriptomic atlas of aged human microglia. *Nat Commun* **9**, 539 (2018).

42. Clarke, L. E. *et al.* Normal aging induces A1-like astrocyte reactivity. *Proc. Natl. Acad. Sci. U.S.A.* **115**, E1896–E1905 (2018).

43. Magistretti, P. J. & Allaman, I. A cellular perspective on brain energy metabolism and functional imaging. *Neuron* **86**, 883–901 (2015).

44. Kuzawa, C. W. *et al.* Metabolic costs and evolutionary implications of human brain development. *Proc. Natl. Acad. Sci. U.S.A.* **111**, 13010–13015 (2014).

45. Pellerin, L. & Magistretti, P. J. Glutamate uptake into astrocytes stimulates aerobic glycolysis: a mechanism coupling neuronal activity to glucose utilization. *Proc. Natl. Acad. Sci. U.S.A.* **91**, 10625–10629 (1994).

46. Pellerin, L. & Magistretti, P. J. Sweet sixteen for ANLS. *J. Cereb. Blood Flow Metab.* **32**, 1152–1166 (2012).

47. Alberini, C. M., Cruz, E., Descalzi, G., Bessières, B. & Gao, V. Astrocyte glycogen and lactate: New insights into learning and memory mechanisms. *Glia* **66**, 1244–1262 (2018).

48. Boisvert, M. M., Erikson, G. A., Shokhirev, M. N. & Allen, N. J. The Aging Astrocyte Transcriptome from Multiple Regions of the Mouse Brain. *Cell Rep* **22**, 269–285 (2018).

49. Tremblay, M.-È. *et al.* The role of microglia in the healthy brain. *J. Neurosci.* **31**, 16064–16069 (2011).

50. Kettenmann, H., Hanisch, U.-K., Noda, M. & Verkhratsky, A. Physiology of microglia. *Physiol. Rev.* **91**, 461–553 (2011).

51. Safaiyan, S. *et al.* Age-related myelin degradation burdens the clearance function of microglia during aging. *Nat. Neurosci.* **19**, 995–998 (2016).

52. Glasser, M. F. & Van Essen, D. C. Mapping human cortical areas in vivo based on myelin content as revealed by T1- and T2-weighted MRI. *J. Neurosci.* **31**, 11597–11616 (2011).

53. Elston, G. N. & Fujita, I. Pyramidal cell development: postnatal spinogenesis, dendritic growth, axon growth, and electrophysiology. *Front Neuroanat* **8**, 78 (2014).

54. la Fougère, C. *et al.* Where in-vivo imaging meets cytoarchitectonics: the relationship between cortical thickness and neuronal density measured with high-resolution [18F]flumazenil-PET. *Neuroimage* **56**, 951–960 (2011).

55. Wagstyl, K., Ronan, L., Goodyer, I. M. & Fletcher, P. C. Cortical thickness gradients in structural hierarchies. *Neuroimage* **111**, 241–250 (2015).

56. Wen, J., Goyal, M. S., Astafiev, S. V., Raichle, M. E. & Yablonskiy, D. A. Genetically defined cellular correlates of the baseline brain MRI signal. *Proc. Natl. Acad. Sci. U.S.A.* **115**, E9727–E9736 (2018).

57. Krogsrud, S. K. *et al.* Development of hippocampal subfield volumes from 4 to 22 years. *Hum Brain Mapp* **35**, 5646–5657 (2014).

58. Tamnes, C. K. *et al.* Intellectual abilities and white matter microstructure in development: a diffusion tensor imaging study. *Hum Brain Mapp* **31**, 1609–1625 (2010).

59. Fjell, A. M. *et al.* The relationship between diffusion tensor imaging and volumetry as measures of white matter properties. *Neuroimage* **42**, 1654–1668 (2008).

60. Sneve, M. H. *et al.* Mechanisms underlying encoding of short-lived versus durable episodic memories. *J. Neurosci.* **35**, 5202–5212 (2015).

61. Engvig, A. *et al.* Effects of memory training on cortical thickness in the elderly. *Neuroimage* **52**, 1667–1676 (2010).

62. de Lange, A.-M. G. *et al.* White matter integrity as a marker for cognitive plasticity in aging. *Neurobiol. Aging* **47**, 74–82 (2016).

63. Folstein, M. F., Folstein, S. E. & McHugh, P. R. 'Mini-mental state'. A practical method for grading the cognitive state of patients for the clinician. *J Psychiatr Res* **12**, 189–198 (1975).

64. Beck, A. & Steer, R. *Beck depression inventary scoring manual*. (Psychologi. ed New York: Psychological., 1987).

65. Salum, G. A. *et al.* High risk cohort study for psychiatric disorders in childhood: rationale, design, methods and preliminary results. *Int J Methods Psychiatr Res* **24**, 58–73 (2015).

66. Pausova, Z. *et al.* Cohort Profile: The Saguenay Youth Study (SYS). *Int J Epidemiol* **46**, e19 (2017).

67. Ellis, K. A. *et al.* The Australian Imaging, Biomarkers and Lifestyle (AIBL) study of aging: methodology and baseline characteristics of 1112 individuals recruited for a longitudinal study of Alzheimer's disease. *Int Psychogeriatr* **21**, 672–687 (2009).

68. Reuter, M., Schmansky, N. J., Rosas, H. D. & Fischl, B. Within-subject template estimation for unbiased longitudinal image analysis. *NeuroImage* **61**, 1402–1418 (2012).

69. Dale, A. M., Fischl, B. & Sereno, M. I. Cortical surface-based analysis. I. Segmentation and surface reconstruction. *Neuroimage* **9**, 179–194 (1999).

70. Fischl, B., Sereno, M. I. & Dale, A. M. Cortical surface-based analysis. II: Inflation, flattening, and a surface-based coordinate system. *Neuroimage* **9**, 195–207 (1999).

71. Fischl, B. & Dale, A. M. Measuring the thickness of the human cerebral cortex from magnetic resonance images. *Proc. Natl. Acad. Sci. U.S.A.* **97**, 11050–11055 (2000).

72. Wood, S. N. *Generalized additive models: an introduction with R*. (Chapman Hall/CRC, 2006).

73. Fjell, A. M. *et al.* Critical ages in the life course of the adult brain: nonlinear subcortical aging. *Neurobiol. Aging* **34**, 2239–2247 (2013).

74. French, L. & Paus, T. A FreeSurfer view of the cortical transcriptome generated from the Allen Human Brain Atlas. *Front Neurosci* **9**, 323 (2015).

75. Miller, J. A. *et al.* Transcriptional landscape of the prenatal human brain. *Nature* **508**, 199–206 (2014).

76. O'Leary, N. A. *et al.* Reference sequence (RefSeq) database at NCBI: current status, taxonomic expansion, and functional annotation. *Nucleic Acids Res.* **44**, D733-745 (2016).

77. Colantuoni, C. *et al.* Temporal dynamics and genetic control of transcription in the human prefrontal cortex. *Nature* **478**, 519–523 (2011).

78. Trabzuni, D. *et al.* Quality control parameters on a large dataset of regionally dissected human control brains for whole genome expression studies. *J. Neurochem.* **119**, 275–282 (2011).

79. GTEx Consortium. Human genomics. The Genotype-Tissue Expression (GTEx) pilot analysis: multitissue gene regulation in humans. *Science* **348**, 648–660 (2015).

80. Richardson, J. E. & Bult, C. J. Visual annotation display (VLAD): a tool for finding functional themes in lists of genes. *Mamm Genome* **26**, 567–573 (2015).

81. Yu, G. *et al.* GOSemSim: an R package for measuring semantic similarity among GO terms and gene products. *Bioinformatics* **26**, 976–978 (2010).

Acknowledgments

This work was supported by the Department of Psychology, University of Oslo (to K.B.W., A.M.F.), and the Norwegian Research Council (to K.B.W., A.M.F.). The project has received funding from the Coordenação de Aperfeiçoamento de Pessoal de Nível Superior - Brasil under Finance Code 001 (to A.P.J.), the European Research Council's Starting Grant scheme under grant agreements 283634, 725025 (to A.M.F.) and 313440 (to K.B.W.) and the INTPART programme agreement 261577 (to K.B.W).

Author Contributions

D.V.P, T.P., A.M.F, Z.P., and K.B.W. designed the study; A.P.J., G.S., and AIBL collected data; D.V.P, N.P., J.S., L.F., A.M.M., Y.P., and Ø.S. performed the analyses, created the figures. The paper was written by D.V.P, T.P. and, A.M.F with input from all the authors.

Competing Interests statement

The authors declare no conflicts of interest.